Journal of Thermal Analysis and Calorimetry, Vol. 96 (2009) 2, 607–615

SPECTRAL, THERMAL AND BIOLOGICAL ACTIVITY STUDIES ON RUTHENIUM(II) COMPLEXES WITH SOME PYRIDYLAMINES

M. M. Omar[*]

Chemistry Department, Faculty of Science, Cairo University, Giza, Egypt

Complexes resulted from the interaction of $[Ph_3P]_3RuCl_2$ with 2-aminoethylpyridine (aepy), 2-hydrazinopyridine (hzpy) and dipicolylamine (dpa) with KPF_6 have been isolated from ethanol. The structures of the complexes were investigated using elemental analyses, IR, magnetic moment, UV-Vis and ^1H NMR spectroscopy. The complexes have been isolated as $[Ru(hzpy)_3](PF_6)_2$, $[Ru(hzpy)_2(aepy)](PF_6)_2$, $[Ru(hzpy)(aepy)_2](PF_6)_2$, $[Ru(dpa)_2](PF_6)_2$ in an octahedral geometry. The thermal decomposition of complexes was discussed in terms of their structures and the thermodynamic parameters were evaluated. The metal complexes were screened for their antibacterial activity against bacterial species, *Escherichia coli*, *Staphylococcus aureus*, as well as fungus (*Candida*). The activity data show the metal complexes have potent antibacterials against one ore more bacterial species.

Keywords: *bacterial activity, ^1H NMR, IR, magnetic moment, pyridylamines complexes, thermal analysis, UV-Vis*

Introduction

The role of ligands in coordination and organometallic chemistry does not need emphatic presentation since their fundamental importance in determining the morphology and the chemical–physical properties of the complexes are well documented by an impressive wealth of literature data. Pyridylamines find a large application in the field of coordination chemistry with different metal ions for their biological, spin transition, organometallic and catalytic activities [1–15]. Hydrazinopyridine (hzpy), aminoethylpyridine (aepy) and dipicolylamine (dpa) are extremely capable ligands for complex formation with metal ions. These ligands, with diamine groups, which might involve some potential antitumour properties, encouraged us to study its reaction with different metal ions. The present study aims to synthesize and investigate the structures of the new complexes obtained from the reaction of $[Ph_3P]_3RuCl_2$ with 2-aminoethylpyridene (aepy), 2-hydrazinopyridine (hzpy) and dipicolylamine (dpa). The thermal analysis is an important tool in studying the thermal stability and the kinetics of complexes [16–20], hence the thermal decompositions and their kinetics were studied.

Experimental

Materials

$[Ph_3P]_3RuCl_2$ and a2-(2-aminoethyl)pyridine, hzpy and dpa were supplied from Aldrich. All solvents were of analytical grade and/or were purified by distillation before use.

Synthesis of $[Ru(hzpy)_3](PF_6)_2$ complex

A mixture of 1.0 mmol of $[Ph_3P]_3RuCl_2$ (0.96 g), 3.0 mol of 2-hydrazinopyridine (0.3273 g) and 3.0 mmol of KPF_6 (0.5522 g) were degassed by N_2 and stirred for 1 h where a dark blue precipitate was separated [16]. The isolated solid was recrystallized from ethyl alcohol, filtered and washed thoroughly with ethanol and then diethyl ether and dried under vacuum.

Synthesis of $[Ru(hzpy)_2(aepy)](PF_6)_2$ complex

A mixture of 1.0 mmol of $[Ph_3P]_3RuCl_2$ (0.96 g), 2.0 mol of 2-hydrazinopyridine (0.2182 g) and 1.0 mmol of 2-(2-aminoethyl)pyridine (0.1222 g) and 3.0 mmol of KPF_6 (0.5522 g) were degassed by N_2 and stirred for 1 h where a dark blue precipitate was separated. The isolated solid was recrystallized from ethyl alcohol, filtered and washed thoroughly with ethanol and then diethyl ether and dried under vacuum.

Synthesis of $[Ru(hzpy)(aepy)_2](PF_6)_2$ complex

The complex was prepared by the same method as $[Ru(hzpy)_2(aepy)](PF_6)_2$ while the mole ratio mixed were; 1:1:2:3 mmol of $RuCl_3$:hzpy:aepy:KPF6, respectively.

Synthesis of $[Ru(dpa)_2](PF_6)_2$ complex

A mixture of 1.0 mmol of $[Ph_3P]_3RuCl_2$ (0.96 g), 2.0 mol of dipicolylamine (0.3986 g) and 3.0 mmol of KPF_6 (0.5522 g) were degassed by N_2 and stirred for 1 h where a dark blue precipitate was separated. The isolated solid was recrystallized from ethyl alco-

* mmomar27@yahoo.com

1388–6150/$20.00

Akadémiai Kiadó, Budapest, Hungary
Springer, Dordrecht, The Netherlands

hol, filtered and washed thoroughly with ethanol and then diethyl ether and dried under vacuum.

Determination of order of the decompostion reaction

The mass fraction of the material (C_s) at the DTG peak temperature (T_{max}) is calculated from the Horowitz and Metzger equation [17]:

$$C_s = \frac{W_s - W_f}{W_0 - W_f} \quad (1)$$

where W_s stands for the mass remaining at a given temperature T_{max}, i.e. the DTG peak temperature, W_0 is the initial mass of the material and W_f is the final mass of the material. Then, the order of the decomposition reaction (n) can be calculated from the following relation:

$$C_s = n^{1/(1-n)} \quad (2)$$

Instrumental methods

Elemental analyses (C, H, N) were made at the Microanalytical Center at Cairo University; the analyses have been repeated twice. The IR spectra have been recorded on a PerkinElmer FT-IR type 1650 spectrophotometer in wavenumber region 4000–200 cm^{-1}. The spectra were recorded as KBr discs. UV-Vis measurements were performed using 1201 spectrophotometer (Shimadzu); in the wavelength range 200–900 nm. ^1H NMR spectra were recorded using 300 MHz Varian-oxford Mercury. The samples were dissolved in deuterated DMSO using TMS as an internal reference. The molar magnetic susceptibilities were measured on powdered samples (Gouy method) using a Sherwood Scientific magnetic susceptibility balance.

Thermal analysis of the complexes were carried out using a Shimadzu thermogravimetric analyzer TGA-50H in a dynamic nitrogen atmosphere (flow rate 20 mL min^{-1}) with a heating rate of 10°C min^{-1}. The mass loss % was measured from the ambient temperature up to 1000°C.

Calculation of kinetic and thermodynamic parameters

Integral method using the Coats–Redfern equation

For a first order process the Coats–Redfern equation [18] may be written in the form:

$$\log \frac{\log(W_\infty / W_r)}{T^2} = \log\left[\frac{AR}{\theta E^*}\left(1 - \frac{2RT}{E^*}\right)\right] - \frac{E^*}{2.303RT} \quad (3)$$

where W_∞ is the mass loss at the completion of the reaction, W_r is the mass loss up to temperature T; ($W_r = W_\infty - W$), W is the mass loss up to temperature T, R is the gas constant, E^* is the activation energy in J mol^{-1} and θ is the heating rate.

Since $1 - 2RT/E^* \cong 1$, a plot of the left hand side of Eq. (3) *vs*. $1/T$ was drawn which gave straight lines where the activation energy E^* and A (Arrhenius constant) were calculated from the slope and the intercept, respectively.

Approximation method using HM equation

For the first order kinetic process, the Horowitz–Metzger equation [17] may be written in the form:

$$\log\left(\log \frac{W_\infty}{W_r}\right) = \frac{\theta E^*}{2.303RT_{max}^2} - \log 2.303 \quad (4)$$

where T_{max}=DTG peak temperature and $\theta = T - T_{max}$. A plot of $\log[\log(W_c/W_r)]$ *vs*. θ will give a straight line and ΔE^* can be calculated from the slope.

The activation energy E^* was calculated from both the Coats–Redfern and the Horowitz–Metzger equations, and then the average of these two values was used to calculate the in the activation enthalpy H^* using the following equation:

$$H^* = E^* - RT \quad (5)$$

where R is the gas constant (R=8.314 J mol^{-1} K^{-1}), T_{max}=DTG peak temperature, which is the maximum decomposition rate temperature.

The activation entropy S^* and the free energy of activation G^* were calculated using the following equations:

$$S^* = 2.303\left(\log \frac{Ah}{KT}\right)R \quad (6)$$

$$G^* = H^* - T_s S^* \quad (7)$$

Biological activity

A 0.5 mL spore suspension (10^{-6}–10^{-7} spore mL^{-1}) of each of the investigated organisms was added to a sterile agar medium just before solidification, then poured into sterile petri dishes (9 cm in diameter) and left to solidify. Using sterile cork borer (6 mm in diameter), three (wells) were made in each dish, then 0.1 mL of the tested compounds dissolved in DMSO (20 mg mL^{-1}) were poured into these holes. Finally, the dishes were incubated at 37°C for 48 h where clear or inhibition zones were detected around each hole. 0.1 mL DMSO alone was used as a control under the same condition for each organism and by subtracting the diameter of inhibition zone resulting with DMSO

from the obtained in each case, both antibacterial activity can be calculated as a mean of three replicates [19].

Results and discussion

The complexes formed from $[Ph_3P]_3RuCl_2$ and aepy, hzpy and dpa in ethanol were prepared. The complexes were subjected to elemental analysis, spectral and magnetic investigations to elucidate their structures. The results of elemental analyses of the isolated complexes are listed in Table 1. A good agreement between the experimental and the calculated values was observed.

Infrared measurements

The IR spectra of the pyridine ligands; Table 2, showed medium to strong band(s) at 3420–3363 and 3308–3287 cm^{-1} which are assigned to the stretching vibration of the NH_2(aepy and hzpy) or NH(dpa) groups. These bands have been found shifted to lower frequencies in the spectra of all complexes which indicate the coordination of these groups to metals [15, 20]. The coordination of the NH_2 or NH groups is also confirmed from the shift of their deformation vibration found at 1285–1207 (ρ_tNH_2), 1150–1048 (ρ_wNH_2) and 769–759 cm^{-1} (ρ_rNH_2) to higher frequencies in the spectra of complexes to be at 1326–1251, 1155–1150 and 781–772 cm^{-1} [15, 20]. The pyridine (py) vibrations in the higher frequency region are not shifted appreciably upon complexation, whereas those at 610–604 cm^{-1} (in-plane ring deformation) and 415–406 cm^{-1} (out-of-plane ring deformation) are found to be shifted in the spectra of complexes to higher frequencies; 658–640 and 467–436 cm^{-1}, respectively [15, 20, 21]. New bands appeared in the spectra of all complexes in the range 569–545 cm^{-1} which are assigned to the ν_{M-N} vibrations.

UV-Vis studies

The UV-Vis spectra of the ligands; Table 1, displayed two main absorption bands at 370–312 and 279–266 nm which may be assigned to n–π^* and π–π^* transition within the pyridine nuclei [15]. The former one was found shifted in the spectra of all complexes indicating that the n–π^* is affected by the coordination of the pyridine nitrogen to ruthenium. In addition, the complexes displayed new absorption band at 645–501 nm which may be assigned to d–d transition within the octahedral arrangement [20].The shifts in the maximum absorption of the $[Ru(hzpy)_2(aepy)](PF_6)_2$ and $[Ru(hzpy)(aepy)_2](PF_6)_2$ to higher wavelengths; 645–528 nm (lower energy; 15504–18939 cm^{-1}) compared with the 514 nm (19455 cm^{-1}) of the $[Ru(hzpy)_3](PF_6)_2$ reflect the strong octahedral field produced by the bonding of three hzpy ligands with more electron rich hydrazine group. This field strength is decreased by subsequent replacement of the hydrazine group by less electron rich ethylamino groups of the aepy ligands. This finding can be with-

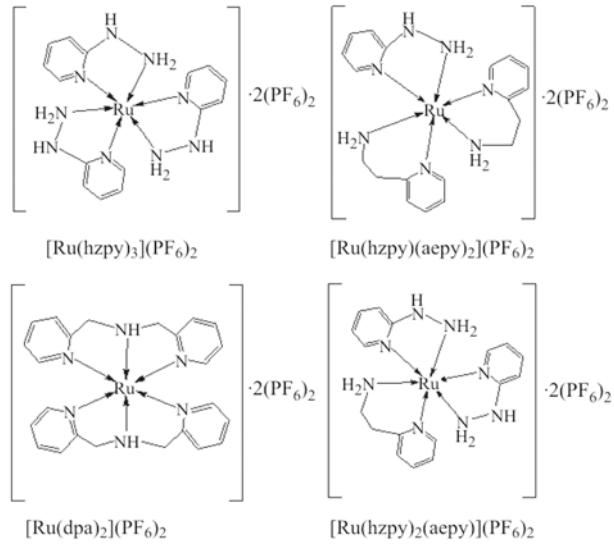

Scheme 1 Structures of ruthenium(II) complexes

Table 1 Elemental analysis and UV-Vis spectral data of complexes

Compound	Molecular mass	C/%	H/%	N/%	UV-Vis*, λ_{max}/nm (Δ_{oct}/cm^{-1})
		found (calcd.)			
$[Ru(hzpy)_3](PF_6)_2$	718.39	25.77 (25.08)	2.93 (2.95)	17.31 (17.55)	514 (19455) 288sh
$[Ru(hzpy)_2(aepy)](PF_6)_2$	731.42	27.22 (27.92)	3.27 (3.31)	15.29 (15.32)	528 (18939), 374sh
$[Ru(hzpy)(aepy)_2](PF_6)_2$	744.46	30.64 (30.65)	3.62 (3.66)	13.08 (13.17)	645 (15504), 388
$[Ru(dpa)_3](PF_6)_2$	789.50	35.73 (36.51)	3.30 (3.32)	9.93 (10.16)	501 (19960), 375

*λ_{max}: aepy: 342, 279, hzpy: 312 sh, 266, dpa: 370, 279, nm, sh: shoulder

drawn also to the $[Ru(dpa)_2](PF_6)_2$ which was found to have the highest ligand field (501 nm, 19960 cm^{-1}). This is expected with two tridentate ligands (dpa's) which form with ruthenium four chelate rings compared with three rings formed by hzpy and/or aepy in the former complexes (Scheme 1).

Diamagnetism of complexes

The magnetic moments of all complexes fell into zero indicating the diamagnetic nature of these complexes. The diamagnetism of the isolated ruthenium complexes have been further confirmed from the ^1H NMR spectral measurements of $[Ru(hzpy)(aepy)_2](PF_6)_2$ complex. The hzpy and aepy ligands displayed multiplets at 8.62–7.23 with 4 protons (aepy, hzpy) assigned for the aromatic protons of the pyridine ring, Table 2. In addition, aminoethylpyridine (aepy) showed two doublets at 3.14 ppm and 2.98 with an integration of 4 protons, assigned to the two CH_2 protons. It displayed also singlet at 2.0 assigned to NH_2 protons. The 2-hydrazinopyridine displayed two additional singlets at 4.0 and 2.0 ppm with integration corresponding to one and two protons which can be assigned to NH and NH_2 protons; respectively. $[Ru(hzpy)(aepy)_2](PF_6)_2$ complex showed multiplet peaks in the range 6.8–9.5 ppm with integration of 12 protons which may be assigned to the pyridine ring protons. The complex showed also three peaks in the range 3.4–4.3 ppm. The first singlet at 4.3 ppm (1 proton) can be assigned to the NH proton of the hzpy ligand while the other two multiplet peaks found at 3.43–3.93 ppm (8 protons) may be assigned to the four methylenes (CH_2) of the two aepy ligands. The peaks due to the three NH_2 (with integration of 6 protons) were found in the range 1.03–1.93 ppm.

The diamagnetic nature of the complexes can be explained in terms of the low spin d^6 ruthenium(II) complexes with $t_{2g}^6 e_g^0$ configuration [22].

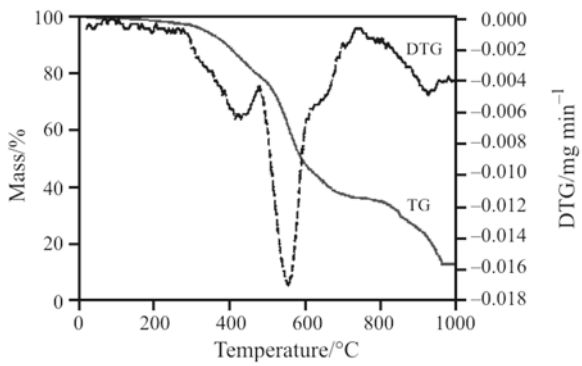

Fig. 1 TG and DTG curves of the thermal decomposition of $[Ru(hzpy(aepy)_2](PF_6)_2$ complex

Thermal analyses

The thermal studies of the ruthenium complexes were carried out using the thermogravimetric TG and the differential thermogravimetric DTG. The thermal data was represented by Fig. 1 while the temperature ranges of decompositions along with the corresponding mass loss of species for all steps are given in Table 3.

$[Ru(hzpy)_3](PF_6)_2$ was thermally decomposed in four successive decomposition steps within the temperature range 50–1000°C. The first decomposition step with an estimated mass loss of 2.36% (calc. mass=17) within the temperature range 50–138°C, may be attributed to the liberation of the NH_3 molecule. The second decomposition step found in the range of 138–258°C with an estimated mass loss of 5.30% (calc. mass=38) may be corresponded to the removal of F_2 molecule. The third decomposition step found within the temperature range 258–617°C with an estimated mass losses of 60.56% (calc. mass losses 436) which is reasonably accounted for by the decomposition of the organic ligands (hzpy's) along with part of the inorganic counter ion as PF_5. The rest of the inorganic counter ion is removed in the fourth step as PF_5 in a wider temperature range 617–990 with a mass loss of 17.58% (calc. mass loss=126). Ruthenium metal (Ru) was remained at the end of decomposition as the metallic residue (14.06%; mass=101) [15].

$[Ru(hzpy)_2(aepy)](PF_6)_2$ decomposed in five decomposition steps within the temperature range 50–700°C. The first two decomposition steps are very close (50–114, 114–138°C) with a total estimated mass loss of 14.85% (calc. mass=109) may be attributed to the removal a hzpy ligand. The rest of the organic matter is removed in the third and the fourth decomposition steps (138–314, 394–571°C) with mass losses of 21.90 and 14.95% corresponding to (aepy+F_2) and hzpy, respectively. The inorganic matter is removed in the fifth step (571–700°C) as PF_5 leaving ruthenium metal as the metallic residue (mass remained=13.87%).

$[Ru(hzpy)(aepy)_2](PF_6)_2$ decomposed in three well separated steps within the temperature range 276–990°C. The first decomposition step found in the temperature range 276–480 with mass loss of 21.28% (calc. mass=158.42) which may be assigned to the removal of aepy ligand along with F_2 gas. The second decomposition step found in the temperature range 480–613°C with a mass loss of 48.02% is corresponded to the removal of hzpy, aepy and part of the inorganic matter as PF_5. The rest of the associated counter ion is removed in the fourth step (742–990°C, mass loss 16.95%) as PF_5 leaving ruthenium metal as the metallic residue (mass remained 13.64%).

$[Ru(dpa)_2](PF_6)_2$ decomposed in five decomposition steps within the temperature range of 50–926°C.

Table 2 IR and ^{1}H NMR data of the ligands and their complexes

Compound	ν_{NH_2}	ρ_{NH_2}	py	ν_{M-N}	^{1}H NMR/ppm
aepy	3363s, 3287s	1207m, 1150m, 760s	604w, 415w	–	7.67–7.23m (4H, pyridine), 3.14–2.98 (4H, ethyl), 2.0s (2H, NH_2)
hzpy	3420b, 3306b	1285, 1020, 769	608w, 406w	–	8.11–6.60m (4H, pyridine), 4.0s (1H, NH), 2.0s (H, NH_2)
dpa	3400s, 3308s	1225, 1048, 759	610w, 412w	–	
$[Ru(hzpy)_3](PF_6)_2$	3316m, 3120m	1326m, 1154m, 772m	650w, 450w	545w	
$[Ru(hzpy)_2(aepy)](PF_6)_2$	3306b, 3120b	1252w, 1155m, 781w	658m, 467w	569m	
$[Ru(hzpy)(aepy)_2](PF_6)_2$	3325sh, 3100m	1253m, 1152w, 774w	640w, 460w	561m	6.82–9.59m (12H, pyridine), 4.3s (1H, NH), 3.43–3.93 2m (8H, $4CH_2$), 1.03–1.93m (6H, $3NH_2$)
$[Ru(dpa)_2](PF_6)_2$	3340b, 3112b	1251m, 1150w, 772m	640w, 436m	559m	

s: strong, m: medium, mb: medium broad., w: weak

Table 3 Thermoanalytical results (TG) and mass spectrometry data for ruthenium complexes

Complex	F. mass	TG range/°C	DTG_{max}/°C	Mass loss/% found (calcd.)	Assignment of the removed species	Metallic residue/% found (calcd.)
$[Ru(hzpy)_3](PF_6)_2$	718.39	50–138	59	2.36 (2.37)	loss of NH_3	Ru 14.06 (14.11)
		138–258	197	5.30 (5.29)	loss of F_2	
		258–617	400	60.56 (60.69)	loss of 3hzpy–NH_3+PF_5	
		617–990	954	17.58 (17.54)	loss of PF_5	
$[Ru(hzpy)_2(aepy)](PF_6)_2$	731.42	50–114, 114–138	86, 123	14.85 (14.95)	loss of hzpy	2Ru 13.81 (13.87)
		138–314	207	21.90 (21.88)	loss of aepy+F_2	
		394–571	531	14.95 (14.90)	loss of hzpy	
		571–700	642	34.38 (34.45)	loss of 2PF_5	
$[Ru(hzpy)(aepy)_2](PF_6)_2$	744.46	276–480	429	21.28 (21.49)	loss of aepy+F_2	Ru 13.64 (13.57)
		480–613	558	48.02 (47.95)	loss of hzpy+aepy+PF_5	
		742–990	930	16.95 (16.93)	loss of PF_5	
$[Ru(dpa)_3](PF_6)_2$	789.50	50–102	63	4.80 (4.83)	loss of F_2	Ru 12.65 (12.79)
		102–213	157	9.89 (10.00)	loss of py	
		213–451	322	22.95 (23.31)	loss of 2py+C_2H_2	
		451–636	562	17.87 (17.35)	loss of py+2CH=NH	
		636–926	807	31.84 (31.92)	2PF_5	

py=pyridine moiety

Table 4 Kinetic data of the thermal decomposition of ruthenium complexes

Compound	Decomp. steps/°C	DTG_{max}/°C	E^*/kJ mol^{-1}			R^2		S/s^{-1}	H^*/kJ mol^{-1}	G^*/kJ mol^{-1}	Cs
			CR	HM	mean	CR	HM				
$[Ru(hzpy)_3](PF_6)_2$	50–138	59	23.06	25.59	24.33	0.99	0.99	–189	21.61	83.46	0.29
	138–258	197	60.39	68.74	64.57	0.97	0.97	–126	60.67	119.88	0.31
	258–617	400	55.26	60.57	57.92	0.97	0.94	–188	52.30	179.41	0.32
	617–990	954	29.83	34.69	32.26	0.96	0.96	–14	312.41	321.19	0.34
					179.08						
$[Ru(hzpy)_2(aepy)](PF_6)_2$	50–138	123	34.30	42.85	38.58	0.92	0.94	–172	34.94	110.08	0.26
	138–314	207	76.26	70.99	73.63	0.86	0.94	–117	69.62	125.82	0.34
	394–571	531	130.25	152.94	141.60	0.96	0.98	–86	135.10	201.98	0.29
	571–700	642	252.41	258.94	255.68	0.88	0.88	–15	248.20	234.47	0.30
					509.49						
$[Ru(hzpy)(aepy)_2](PF_6)_2$	276–480	429	46.49	67.69	57.09	0.97	0.98	–189	51.28	183.50	0.32
	480–613	558	119.89	117.48	118.69	0.88	0.88	–133	11.76	222.15	0.33
	742–995	930	226.55	271.60	249.08	0.97	0.96	–66	239.06	318.15	0.31
					424.86						
$[Ru(dpa)_3](PF_6)_2$	50–102	63	52.82	61.97	57.39	0.99	0.98	–87	54.58	83.95	0.27
	102–213	157	29.42	33.91	31.66	0.99	0.99	–196	28.07	112.54	0.34
	213–451	322	59.21	77.84	68.53	0.94	0.94	–148	63.55	152.20	0.33
	451–636	562	105.16	138.51	121.84	0.96	0.97	–120	114.88	215.52	0.28
	636–926	807	123.51	160.28	141.90	0.94	0.94	–138	132.91	281.57	0.33
					421.32						

Table 5 Biological activity of metal complexes

Sample	*Escherichia coli*	*Staphylococcus aureus*	Fungus (*Candida*)
C/mg L^{-1}	2	2	2
$[Ru(hzpy)_3](PF_6)_2$	++	++	–
$[Ru(hzpy)_2(aepy)](PF_6)_2$	++	++	–
$[Ru(hzpy)(aepy)_2](PF_6)_2$	++	++	–
$[Ru(dpa)_2](PF_6)_2$	+++	+++	++
Tetracycline	++++	++++	–
Amphotricine	+++	+++	–

The test was performed using the diffusion agar technique. Inhibition values=up to 10 mm beyond control=+, Inhibition values=11–15 mm beyond control=++, Inhibition values=16–22 mm beyond control=+++ , Inhibition values>23 mm beyond control=++++

The % mass losses of the five decomposition steps found as 4.8, 9.89, 22.95, 17.87 and 31.84 were assigned to the removal of F_2, py, ($2py+C_2H_2$), (py+2CH=NH) and $2PF_5$; respectively. Ruthenium was found as the remaining residue (12.65%).

Kinetics of thermal decomposition

The complexes decomposed in multi-step pattern, the Cs; calculated for each step, fell into the range 0.27–0.34 which indicates that all decompositions follow first order reaction [17, 23]. The thermodynamic parameters were evaluated based on Coats–Redfern and Horowitz–Metzer methods and the mean values obtained for the activation energies and Arrhenius constant were used; for the sake of accuracy, to calculate the other parameters (activation enthalpy (H*) and Gibbs free energy (G*), (Table 4).

The activation energies of the decomposition were sum of 179.08, 509.49, 424.86 and 421.32 kJ mol^{-1} for $[Ru(hzpy)_3](PF_6)_2$, $[Ru(hzpy)_2(aepy)](PF_6)_2$, $[Ru(hzpy)(aepy)_2](PF_6)_2$ and $[Ru(dpa)_2](PF_6)_2$, respectively. These values indicate the thermal stability of the complexes. The decomposition entropy, for the formation of the activated complexes from the starting reactants, is in most cases of negative values. The negative sign of the S* suggests that the degree of structural 'complexity' (arrangement, 'organization') of the activated complexes was higher than that of the starting reactants and the decomposition reactions are slow reactions [24].

Biological activity

All of the tested metal complexes showed a remarkable biological activity against the different types of Gram-positive and Gram-negative bacteria. The data listed in Table 5. On comparing the biological activity of the metal complexes with the standard tetracycline and amphotricine, the following results are obtained:

- The biological activity of the metal complexes are found to be less than that of standard tetracycline and amphotricine except the complex.
- $[Ru(dpa)_2](PF_6)_2$ which has biological activity equal to that of standard amphotricine. The importance of this lies in the fact that these complexes could be applied fairly in the treatment of some common diseases caused by Gram-positive bacterial strains (*Staphyloccus aureus*) and also caused by Gram-negative (*Escherichia coli*). It is found from (Table 5) that the metal complex $[Ru(dpa)_2](PF_6)_2$ has antifungal activity towards *Candida* more than the standard. Therefore, it is claimed here that such complexes might have a possible antitumor effect since Gram-negative bacteria are considered a quantitative microbiological method for testing beneficial and important drugs, in both clinical and experimental tumor chemotherapy [25, 26].

Conclusions

An attempt was made to study the structure of Ru(II) complexes with some pyridylamines. The results suggested that the complexes have an octahedral geometry. The study shows that the thermal decomposition of the complexes follows first order kinetics and the course of thermal decomposition leads finally to Ru metal formation. The study also shows that such complexes might have a possible antitumor effect.

References

1 S. K. Padhi, Thermochim. Acta, 448 (2006) 1.
2 B. Macías, M. V. Villa, M. Salgado, J. Borrás, M. González-Álvarez and F. Sanz, Inorg. Chim. Acta, 359 (2006)1465.
3 S. Mundwiler, R. Waibel, B. Spingler, S. Kunze and R. Alberto, Nuclear Med. Biol., 32 (2005) 473.
4 C. Müller, C. Dumas, U. Hoffmann, P. A. Schubiger and R. Schibli, J. Organomet. Chem., 689 (2004) 4712.

5 A. Mokhir, R. Stiebing and R. Kraemer, Bioorg. Med. Chem. Lett., 13 (2003) 1399.
6 G. Baranovi, Chem. Phys. Lett., 369 (2003) 668.
7 M. Machuqueiro and T. Darbre, J. Inorg. Biochem., 94 (2003) 193.
8 D. Choquesillo-Lazarte, B. Covelo, J. M. González Pérez, A. Castiñeiras and J. N. Gutiérrez, Polyhedron, 21 (2002) 1485.
9 U. Brand and H. Vahrenkamp, Inorg. Chim. Acta, 308 (2000) 97.
10 C. Stern, F. Franceschi, E. Solari,C. Floriani, N. Re and R. Scopelliti, J. Organomet. Chem., 593–594 (2000) 86.
11 H. Chaouk and M. T. W. Hearn, J. Chromatogr. A, 852 (1999) 105.
12 Y. Gultneh, A. R. Khan, D. Blaise, S. Chaudhry, B. Ahvazi, B. B. Marvey and R. J. Butcher, J. Inorg. Biochem., 75 (1999) 7.
13 S. Tachiyashiki and K. Mizumachi, Coord. Chem. Rev., 132 (1994) 113.
14 C. P. Köhler, R. Jakobi, E. Meissner, E. Wiehl, H. Spiering and P. Gütlich, J. Phys. Chem. Solids, 51 (1990) 239.
15 A. A. Soliman, M. M. Khattab and R. M. Ramadan, Trans. Met. Chem., 32 (2007) 325.
16 P. Pearson, A. M. Bond, G. B. Deacon, C. Forsyth and L. Spiccia, Inorg. Chim. Acta, 361 (2008) 601.
17 H. H. Horowitz and G. Metzer, Anal. Chem., 35 (1963) 1464.
18 A. W. Coats and J. P. Redfern, Nature, 201 (1964) 68.
19 N. Sari, S. Arslan, E. Logoglu and I. Sakiyan, J. Sci., 16 (2003) 283.
20 A. A. Soliman, M. M. Khattab and Wolfgang Linert, J. Coord. Chem., 61 (2008) 2017.
21 K. Nakamoto, Infrared and Raman Spectra of Inorganic and Coordination Compounds, 4th Ed., Wiley, New York 1986.
22 C. E. Housecroft and A. G. Sharpe, Inorganic Chemistry, 2nd Ed., Pearson Education Ltd, Essex CM20 2JE, England 2005.
23 A. A. Soliman, S. M. El-Medani and O. A. M. Ali, J. Therm. Anal. Cal., 83 (2006) 385.
24 L. T. Valaev and G. G. Gospodinov, Thermochim. Acta, 370 (2001) 15.
25 A. M. S. El-Sharief, M. S. Ammar and Y. A. Mohammed, Egypt. J. Chem., 27 (1984) 535.
26 G. G. Mohamed, M. M. Omar and A. M. Hindy, Turk. J. Chem., 30 (2006) 361.

Received: June 20, 2008
Accepted: October 13, 2008
Online First: February 4, 2009

DOI: 10.1007/s10973-008-9342-2